Intense up-conversion emissions of Yb^{3+}/Dy^{3+} co-doped Al_2O_3 nanopowders prepared by non-aqueous sol–gel method*

Li Cheng-Ren(李成仁)[a)†], Li Shu-Feng(李淑凤)[b)], Dong Bin(董 斌)[c)], Sun Jing-Chang(孙景昌)[a)], Bo Xiao-Feng(卜晓峰)[a)], and Fan Xu-Nan(范旭楠)[a)]

[a)] *College of Physics and Electronic Technology, Liaoning Normal University, Dalian* 116029, *China*

[b)] *School of Physics and Optoelectronic Technology, Dalian University of Technology, Dalian* 116024, *China*

[c)] *School of Physics and Materials Engineering, Dalian Nationalities University, Dalian* 116600, *China*

(Received 7 January 2012; revised manuscript received 6 April 2012)

Yb^{3+}/Dy^{3+} co-doped Al_2O_3 nanopowders have been prepared by the non-aqueous sol–gel method and their up-conversion photoluminescence spectra are measured under excitation by 980-nm semiconductor laser. The results show that there are comparatively abundant spectra of up-conversion emissions centered at 378, 408, 527 and 543, and 663 nm, corresponding to $^4G_{9/2} \rightarrow {}^6H_{13/2}$, $^4G_{9/2} \rightarrow {}^6H_{11/2}$, $^4I_{15/2} \rightarrow {}^6H_{13/2}$, and $^4F_{9/2} \rightarrow {}^6H_{11/2}$ transitions of Dy^{3+}, respectively. Two-photon and three-photon processes are involved in ultraviolet, violet, green, and red up-conversion emissions. The energy transition between Yb^{3+} and Dy^{3+} is discussed.

Keywords: Yb^{3+}/Dy^{3+} co-doped Al_2O_3 nanopowders, non-aqueous sol–gel method, photo- luminescence spectra, up-conversion emission

PACS: 78.55.Qr, 38.80.Wr **DOI:** 10.1088/1674-1056/21/9/097803

1. Introduction

During the last decade, the materials doped by rare-earth (RE) ions have been investigated widely because of their comprehensive applications in display devices, high-density optical data reading and storage, optical temperature sensor, and so on.[1−5] In particular, much effort has been focused on the trivalent dysprosium which is utilized potentially in the fields of lasers and solid white LED owing to its abundant energy levels.[6−8] However, the host materials doped with Dy^{3+} ions reported in most literatures are crystal or glassy matrix, and the heat treatment is performed at relatively high temperatures.[9−11] Recently, the sol–gel technology has been frequently used to prepare optical materials because it allows the incorporation of trivalent RE ions inside host materials at room temperature.[12−14] The extensive research of photoluminescence (PL) properties of RE ions (such as Er^{3+} ions) indicates that Al_2O_3 is appropriate to be the host matrix,[15,16] and the non-aqueous sol–gel method is more suitable for preparing Dy^{3+}-doped nanopowders in a wide concentration range.[17] Though the down-conversion of Dy^{3+} ions have been investigated previously, the discussion about up-conversion of Dy^{3+} ions is still an interesting work. In this work, a series of samples of Yb^{3+}/Dy^{3+} co-doped Al_2O_3 nanopowders have been prepared by the non-aqueous sol–gel method. The aim of co-doped sensitizer Yb^{3+} is to enhance PL intensities because of its large absorption cross section at 980 nm.[18,19] The up-conversion PL spectra of the nanopowders, which are pumped by a 980-nm semiconductor laser, are measured. The results show that there are comparatively abundant strong spectra of up-conversion emissions centered at 378, 408, 527 (or 543), and 663 nm, corresponding to $^4G_{9/2} \rightarrow {}^6H_{13/2}$, $^4G_{9/2} \rightarrow {}^6H_{11/2}$, $^4I_{15/2} \rightarrow {}^6H_{13/2}$, and $^4F_{9/2} \rightarrow {}^6H_{11/2}$ transitions of Dy^{3+}, respectively. The mechanism of up-conversion is discussed, and the two-photon and three-photon processes are involved in ultraviolet, violet, green and red up-conversion emissions.

*Project supported by the National Natural Science Foundation of China (Grant No. 11004092) and the Scientific Research Fund of Education Department of Liaoning Province, China (Grant No. 2009A417).

†Corresponding author. E-mail: lshdg@sina.com.cn

© 2012 Chinese Physical Society and IOP Publishing Ltd

2. Experimental details

The xYb^{3+}–0.1 mol% Dy^{3+} (x = 0.3, 0.5, and 0.9 mol%) and 0.9 mol% Yb^{3+}–yDy^{3+} (y = 0.1, 0.3, and 0.5 mol%) co-doped Al_2O_3 nanopowders have been prepared using the non-aqueous sol–gel method by the hydrolysis and polycondensation of aluminum isopropoxide [$Al(OC_3H_7)_3$] from pure aluminum (99.99%) and isopropanol (Pr^iOH).

First, the chelating agent acetylacetone (AcAc) is dripped slowly into the $Al(OC_3H_7)_3$ and Pr^iOH solution with a molar ratio of 1:2 for $Al(OC_3H_7)_3$ and AcAc. The solution is agitated for 1 h and held still for 1 hour at room temperature. The AcAc is used to slow down the hydrolysis speed of $Al(OC_3H_7)_3$ and improve the stability of Al_2O_3 sol. Then, the hydrolysis of the modified precursor is performed with stoichiometric quantities of water under a Pr^iOH environment. The molar ratio between H_2O and $Al(OC_3H_7)_3$ is 0.85:1. The concentration of $Al(OC_3H_7)_3$ in the sol is adjusted to be 30 g·l^{-1} with Pr^iOH. The resulting solution is agitated for 3 h. At the same time, some concentrated nitric acid (HNO_3) is added until the pH value is adjusted to be about 3.0, forming a clear, slightly yellow, and very stable Al_2O_3 sol. The rare-earth ions Dy^{3+} and Yb^{3+} are imported by adding $Dy(NO_3)_3{\cdot}5H_2O$ and $Yb(HO_3)_3{\cdot}5H_2O$ with different concentrations. Further strong agitation is required to last for 16 h at room temperature. The xerogels are obtained after drying the Yb^{3+}/Dy^{3+} co-doped Al_2O_3 solution at 373 K for 8 h to remove the solvent. The xerogels are heated to 823 K and kept for 1 h, and cooled to room temperature naturally. Finally, the samples of the Yb^{3+}/Dy^{3+} co-doped Al_2O_3 sintered are milled into powder, and annealed at 1273 K for 2 h in the air environment.

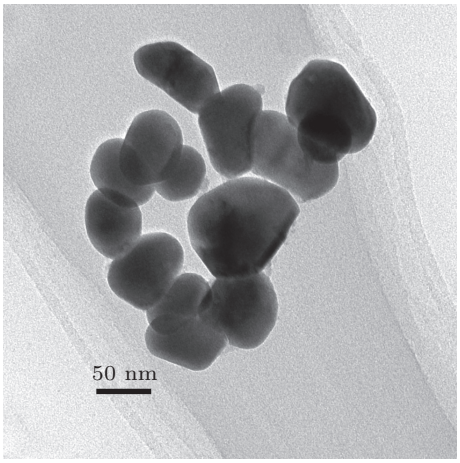


Fig. 1. TEM micrograph of a Yb^{3+}/Nd^{3+} co-doped Al_2O_3 nanoparticle annealed at 1273 K.

Figure 1 shows the transmission electron microscopy (TEM) micrograph of the Yb^{3+}/Nd^{3+} co-doped Al_2O_3 nanoparticles annealed at 1273 K. It can be seen that the average nanoparticle size of Yb^{3+}/Nd^{3+} co-doped Al_2O_3 is about 60 nm, ranging from 40 to 80 nm.

3. Results and discussion

The photoluminescence spectra of Yb^{3+}/Dy^{3+} co-doped Al_2O_3 nanopowders are measured under the excitation of a 980-nm semiconductor laser, as shown in Fig. 2. It can be shown that there are abundant up-conversion emissions centered at 378, 408, 527 and 543, and 663 nm, corresponding to the transitions of $^4G_{9/2} \rightarrow {}^6H_{13/2}$, $^4G_{9/2} \rightarrow {}^6H_{11/2}$, $^4I_{15/2} \rightarrow {}^6H_{13/2}$, and $^4F_{9/2} \rightarrow {}^6H_{11/2}$in Dy^{3+} ions. The intensity at green/red band is obviously higher than that from Yb^{3+}/Er^{3+} co-doped borosilicate glass at the same band, and is close to that of Yb^{3+}/Er^{3+} co-doped oxy–fluoride glass. Especially, the ultraviolet emissions at 378 and 408 nm have never been reported in glassy materials previously.

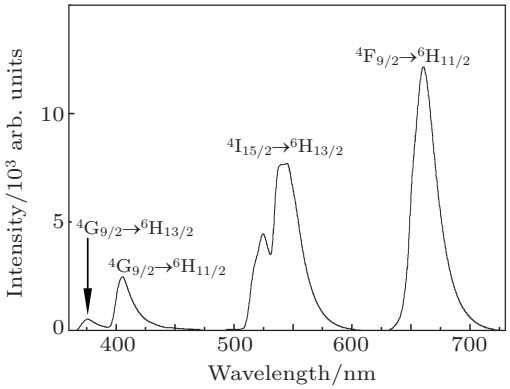


Fig. 2. PL spectrum of 0.9Yb^{3+}–0.3Dy^{3+} (in mol%) co-doped Al_2O_3 powders under 980-nm excitation.

Figure 3 shows the relationship between the photoluminescence intensity and the concentration of Yb^{3+} as well as Dy^{3+}. It can be seen that the PL intensity becomes stronger with the increase of Yb^{3+} concentration, and gets stronger first with the increase of Dy^{3+} concentration, then becomes weaker. This is mainly because that energy is transferred from Yb^{3+} to Dy^{3+}, and the energy transition becomes more active with the increase of Yb^{3+} concentration, resulting in the enhancement of the PL intensity. However, the PL intensity starts to descend because the distances among Dy^{3+} ions are reduced, and the cross

relaxation happens when the Dy^{3+} concentration increases to some extent, leading to the concentration quenching of Dy^{3+}. The composite $0.3Dy^{3+}$–$0.9Yb^{3+}$ (in mol%) is an ideal selection. The inset presents the relationship between the PL intensity and the thermal annealing temperature. The relation curve shows a bell shape, and 1273 K is the optimum temperature.

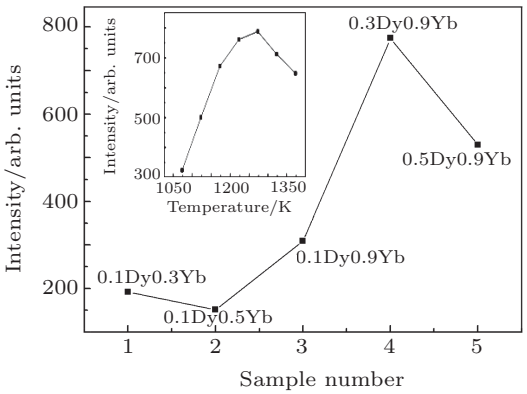


Fig. 3. Relation between PL intensity and the concentration of $x\mathrm{Dy}^{3+}y\mathrm{Yb}^{3+}$.

The spectral shapes do not change with increasing power. Figures 4 and 5 shows the the peak intensities (I_{peak}) of ultraviolet, visible, red, and green up-conversion emissions centered at 378, 408, 527, 543, and 663 nm of Yb^{3+}/Dy^{3+} co-doped Al_2O_3 powder as functions of the pump power. The up-conversion emission intensity (I_{up}) is proportional to the n-th power of the pump power (P_{pump}),[20,21] i.e.,

$$I_{\mathrm{up}} \propto P_{\mathrm{pump}}^{n},$$

where n is the number of photons required to populate the up-conversion emission states. The experimental data of up-conversion emission intensity are fitted into straight lines with a slope of n. It can be seen from Fig. 4 that the slopes are about 3 for both the ultraviolet and violet up-conversion emissions centered at about 378 and 408 nm, indicating

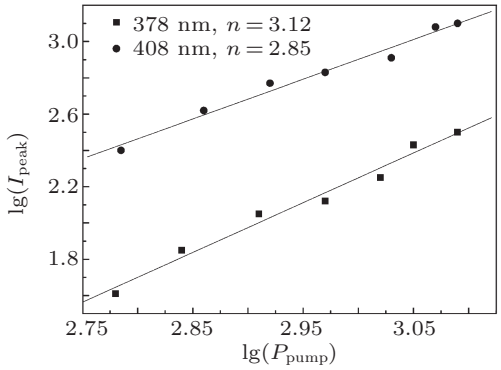


Fig. 4. Peak intensity of the ultraviolet and violet up-conversion emissions as a function of the pump power.

that the three-photon process is involved in the up-conversion emission mechanism for the Yb^{3+}/Dy^{3+} co-doped Al_2O_3 powders. Analogously, the values in Fig. 5 are 2.05, 2.63, and 2.13 for the visible green and red up-conversion emissions centered at about 527, 543, and 663 nm, meaning that two-photon processes are involved.

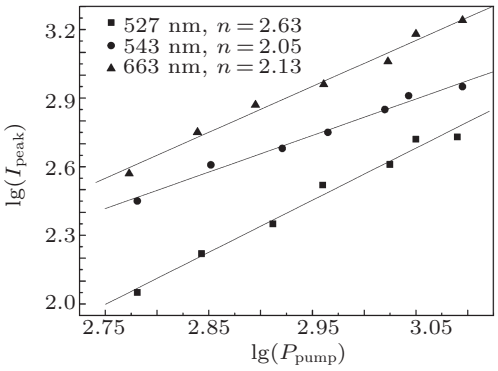


Fig. 5. Dependence of peak intensity of the green and red up-conversion emissions on the pump power.

The diagram of the up-conversion mechanism involved in Yb^{3+}/Dy^{3+} co-doped Al_2O_3 powder is shown in Fig. 6. The ultraviolet up-conversion emissions at 378 and 408 nm are ascribed to the transitions of Dy^{3+} from $^4G_{9/2}$ to $^6H_{13/2}$ and from $^4G_{9/2}$ to $^6H_{11/2}$. Populations at the $^4G_{9/2}$ level are assembled mainly through the ground-state absorption (GSA), the energy transfer (ET) between Yb^{3+} and Dy^{3+}, the excited state absorption (ESA), and the non-radiative decay from high levels to low levels. The detailed processes are listed as follows:

GSA: $(Dy^{3+})\ ^6H_{15/2} + h\nu \rightarrow (Dy^{3+})\ ^6H_{5/2}$,

ET 1: $(Dy^{3+})\ ^6H_{15/2} + (Yb^{3+})\ ^2F_{5/2} \rightarrow (Dy^{3+})\ ^6H_{5/2} + (Yb^{3+})\ ^2F_{7/2}$,

ESA: $(Dy^{3+})\ ^6H_{5/2} + h\nu \rightarrow (Dy^{3+})\ ^4F_{9/2}$,

ET 2: $(Dy^{3+})\ ^6H_{5/2} + (Yb^{3+})\ ^2F_{5/2} \rightarrow (Dy^{3+})\ ^4F_{9/2} + (Yb^{3+})\ ^2F_{7/2}$,

ESA: $(Dy^{3+})\ ^4F_{9/2} + h\nu \rightarrow (Dy^{3+})\ ^4M_{17/2}$,

ET 3: $(Dy^{3+})\ ^4F_{9/2} + (Yb^{3+})\ ^2F_{5/2} \rightarrow (Dy^{3+})\ ^4M_{17/2} + (Yb^{3+})\ ^2F_{7/2}$.

Then, the Dy^{3+} ions at $^4M_{17/2}$ level relax to $^4G_{9/2}$ level. Three-photon process is involved in the discussion.

The red up-conversion photoluminescence at 663 nm comes from the transition $^4F_{9/2} \rightarrow {}^6H_{11/2}$ of Dy^{3+}, and the way how particles accumulate to energy level $^4F_{9/2}$ is given as follows:

GSA: $(Dy^{3+})\ ^6H_{15/2} + h\nu \rightarrow (Dy^{3+})\ ^6H_{5/2}$,

ET 1: $(Dy^{3+})\ ^6H_{15/2} + (Yb^{3+})\ ^2F_{5/2} \rightarrow (Dy^{3+})\ ^6H_{5/2} + (Yb^{3+})\ ^2F_{7/2}$,

ESA: $(Dy^{3+})\ ^6H_{5/2} + h\nu \rightarrow (Dy^{3+})\ ^4F_{9/2}$,

ET 2: (Dy^{3+}) $^6H_{5/2}$ + (Yb^{3+}) $^2F_{5/2}$ → (Dy^{3+}) $^4F_{9/2}$ + (Yb^{3+}) $^2F_{7/2}$.
Obviously, this is two-photon process.

The green up-conversion emissions at 527 and 543 nm come from $^4I_{15/2}$ and its Starks energy split. As for Al_2O_3 matrix, the maximum phonon energy is about 870 cm^{-1}, and the energy level interval between $^4I_{15/2}$ and $^4F_{9/2}$ is about 850 nm^{-1}. Thus, particles are excited to the $^4I_{15/2}$ energy level from $^6H_{5/2}$ in the following ways:

ESA: (Dy^{3+}) $^6H_{5/2}$ + $h\nu$+ a phonon → (Dy^{3+}) $^4I_{15/2}$,

ET 2: (Dy^{3+}) $^6H_{5/2}$ + (Yb^{3+}) $^2F_{5/2}$ + a phonon → (Dy^{3+}) $^4I_{15/2}$ + (Yb^{3+}) $^2F_{7/2}$.

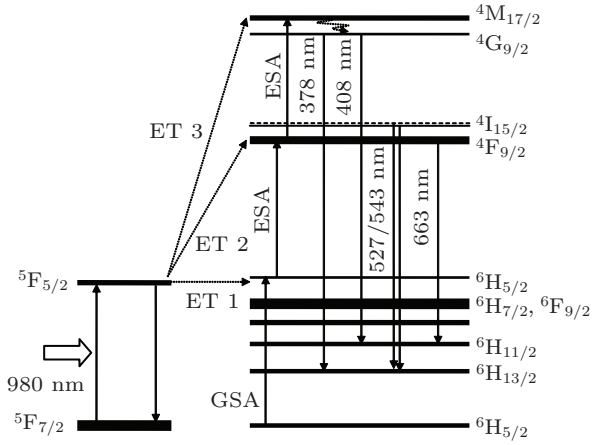


Fig. 6. Energy level diagram of Yb^{3+}/Dy^{3+} co-doped Al_2O_3 powders excited by a 980-nm laser beam.

4. Conclusion

Yb^{3+}/Dy^{3+} co-doped Al_2O_3 nanopowders have been prepared by non-aqueous sol–gel method and detailed technique is introduced. The photoluminescence characteristics of the samples are measured under the excitation of a 980-nm semiconductor laser. There are comparatively abundant strong up-conversion emissions centered at 378, 408, 527 and 543, and 663 nm, respectively, corresponding to the transitions of Dy^{3+} ions: $^4G_{9/2}$ → $^6H_{13/2}$, $^4G_{9/2}$ → $^6H_{11/2}$, $^4I_{15/2}$ → $^6H_{13/2}$ and $^4F_{9/2}$ → $^6H_{11/2}$, and some emissions have never been reported in glassy materials previously. It is also known that PL intensities become weak because the energy is transferred from Dy^{3+} to Yb^{3+} and the concentration quench of Dy^{3+} occurs when the concentration of Dy^{3+} exceeds 0.3 mol%. The power spectra of the Yb^{3+}/Dy^{3+} co-doped Al_2O_3 nanopowders are measured to help analyze the up-conversion mechanism. The three-photon and two-photon processes are found to contribute to ultraviolet, violet, green, and red up-conversion emissions.

References

[1] Li G S, Li C X, Zhang C M, Cheng Z Y, Quan Z W, Peng C and Lin J 2009 *J. Mater. Chem.* **19** 8936

[2] Miura K, Qiu J R, Fujiwara S, Sakaguchi S and Hirao K 2002 *Appl. Phys. Lett.* **80** 2263

[3] Li C R, Dong B, Li S F and Song C L 2007 *Chem. Phys. Lett.* **443** 426

[4] Li J F and Jackson S D 2011 *Chin. Phys.* B **20** 034205

[5] Li C R, Ming C G, Li S F, Ding J H, Wang B C and Zhang L 2008 *Acta Phys. Sin.* **57** 6604 (in Chinese)

[6] Basavapoornima Ch, Jayasankar C K and Chandrchoodan P P 2008 *Pyhsica* B **404** 235

[7] Ci Z P, Wang Y H and Zhang J C 2010 *Chin. Phys.* B **19** 057803

[8] Li P L, Wang Z J, Yang Z P, Guo Q L and Li X 2010 *J. Lumin.* **130** 222

[9] Soares M R N, Soares M J, Fernandes A J S, Rino L, Costa F M and Monteiro T 2011 *J Mater. Chem.* **21** 15262

[10] Seshadri M, Rao K V, Rao J L, Rao K S R K and Ratankaram Y C 2010 *J. Lumin.* **130** 536

[11] Dai S X, Peng B, Le F D, Wang X S, Shen X, Xu T F and Nie Q H 2010 *Acta Phys. Sin.* **59** 3547 (in Chinese)

[12] Dong B, Liu D P, Wang X J, Yang T, Miao S M and Li C R 2007 *Appl. Phys. Lett.* **90** 181117

[13] Wang D W, Zhang D Q, Yuan J, Zhao Q L, Liu H W, Wang Z Y and Cao M S 2009 *Chin. Phys.* B **18** 2596

[14] Wang B C, Li C R, Dong B, Zhang L and Xu W 2009 *Opt. Engine.* **48** 104401

[15] Toudert J, Nunez-Sanchez S, Jimenez C M and Serna R 2008 *Appl. Phys. Lett.* **92** 121111

[16] Singh V, Rai V K, Pak I L, Badie L and Kwak H Y 2009 *Appl. Phys.* B **97** 805

[17] Suriyamurthy N and Bhabani S P 2010 *J. Ameri. Cera. Soci.* **93** 3832

[18] Li C R, Song C L, Li S F, Song Q, Li J Y and Lei M K 2005 *Semicond. Optoelec.* **26** 212 (in Chinese)

[19] Wang X J, Wang B, Wang L, Guo R M, Isshiki H, Kimura T and Zhou Z 2011 *Appl. Phys. Lett.* **98** 071903

[20] Wade S A, Collins S F and Baxter G W 2003 *J. Appl. Phys.* **94** 4743

[21] Li C R, Li S F, Dong B, Cheng Y Q, Yin H T, Yang J and Cheng Y 2011 *Chin. Phys.* B **20** 017803